

2

AD-A261 792



OFFICE OF NAVAL RESEARCH

Contract N00014-91-J-1927

R&T Code 413v001

Technical Report No. 17

HALOGEN ADLAYERS ON AG(111)

by

JOACHIM HOSSICK SCHOTT AND HENRY S. WHITE

Prepared for Publication in

JOURNAL OF THE AMERICAN CHEMICAL SOCIETY

University of Minnesota
Department of Chemical Engineering and Materials Science
Minneapolis, MN 55455

March 20, 1993

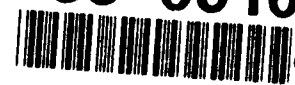
Reproduction in whole or in part is permitted for any purpose of the United States Government.

This document has been approved for public release and sale; its distribution is unlimited.

DTIC
SELECTE
MAR 25 1993
S B D

3 24 042

93-06102
2488



REPORT DOCUMENTATION PAGE

Form Approved
OMB No. 0704-0188

Public reporting burden for this collection of information is estimated to average 1 hour per response, including the time for reviewing instructions, searching existing data sources, gathering and maintaining the data needed, and completing and reviewing the collection of information. Send comments regarding this burden estimate or any other aspect of this collection of information, including suggestions for reducing this burden, to Washington Headquarters Services, Directorate for Information Operations and Reports, 1215 Jefferson Davis Highway, Suite 1204, Arlington, VA 22202-4302, and to the Office of Management and Budget, Paperwork Reduction Project (0704-0188), Washington, DC 20503.

1. AGENCY USE ONLY (Leave blank)		2. REPORT DATE March 20, 1993	3. REPORT TYPE AND DATES COVERED Technical 6/30/92 - 3/31/93	
4. TITLE AND SUBTITLE HALOGEN ADLAYERS ON Ag(111)			5. FUNDING NUMBERS N00014-91-J-1927	
6. AUTHOR(S) JOACHIM HOSSICK SCHOTT AND HENRY S. WHITE				
7. PERFORMING ORGANIZATION NAME(S) AND ADDRESS(ES) Dept. of Chemical Engineering and Materials Science University of Minnesota			8. PERFORMING ORGANIZATION REPORT NUMBER Technical Report No. 17	
9. SPONSORING / MONITORING AGENCY NAME(S) AND ADDRESS(ES) Office of Naval Research 800 North Quincy Street Arlington, VA 22217			10. SPONSORING / MONITORING AGENCY REPORT NUMBER	
11. SUPPLEMENTARY NOTES				
12a. DISTRIBUTION / AVAILABILITY STATEMENT Unclassified/Unlimited			12b. DISTRIBUTION CODE	
13. ABSTRACT (Maximum 200 words) Abstract. Atomically smooth halogen adlayers on Ag(111) (AgX, where X= I, Br, Cl and F) have been prepared by quenching of heated Ag samples in concentrated acid halide (HX) solutions. The AgX adlayers are chemically stable in air for several hours, allowing detailed characterization of the adlayer atomic structures by scanning tunneling microscopy (STM). STM images of I adlayers are consistent with a nearly perfect $\sqrt{3} \times \sqrt{3} / R30$ structure; F, Cl and Br adlayers, however, are characterized by a parallel double row structure of adsorbed halogen atoms, oriented along the [110] direction on the Ag(111) substrate. The row structure observed by STM for Cl and Br adlayers is shown to be consistent with low-energy-electron-diffraction (LEED) patterns, but inconsistent with the corresponding structures derived from LEED. The degree of symmetry in the various adlayers decreases with increasing adatom electronegativity, indicating that the local charge distribution around the adlayer atom, and its size, are the controlling factors in determining the adlayer structure.				
14. SUBJECT TERMS			15. NUMBER OF PAGES 22	
			16. PRICE CODE	
17. SECURITY CLASSIFICATION OF REPORT Unclassified	18. SECURITY CLASSIFICATION OF THIS PAGE UL	19. SECURITY CLASSIFICATION OF ABSTRACT	20. LIMITATION OF ABSTRACT	

Halogen Adlayers on Ag(111)

Joachim Hossick Schott and Henry S. White

Department of Chemical Engineering and Materials Science
University of Minnesota
Minneapolis, MN 55455

Abstract. Atomically smooth halogen adlayers on Ag(111) (AgX, where X= I, Br, Cl and F) have been prepared by quenching of heated Ag samples in concentrated acid halide (HX) solutions. The AgX adlayers are chemically stable in air for several hours, allowing detailed characterization of the adlayer atomic structures by scanning tunneling microscopy (STM). STM images of I adlayers are consistent with a nearly perfect $\sqrt{3}\times\sqrt{3}/R30$ structure; F, Cl and Br adlayers, however, are characterized by a parallel double row structure of adsorbed halogen atoms, oriented along the [110] direction on the Ag(111) substrate. The row structure observed by STM for Cl and Br adlayers is shown to be consistent with low-energy-electron-diffraction (LEED) patterns, but inconsistent with the corresponding structures derived from LEED. The degree of symmetry in the various adlayers decreases with increasing adatom electronegativity, indicating that the local charge distribution around the adlayer atom, and its size, are the controlling factors in determining the adlayer structure.

Submitted to *J. Am. Chem. Soc.*, February 1993

DTIC QUALITY ASSURED 1

1

Accession For	
NTIS GRA&I	<input checked="" type="checkbox"/>
DTIC TAB	<input type="checkbox"/>
Unannounced	<input type="checkbox"/>
Justification _____	
By _____	
Distribution/	
Availability Codes	
Dist	Avail and/or Special
A-1	

Introduction

The nucleation and growth of halogens on silver surfaces is of fundamental interest in surface science¹⁻⁷, interfacial electrochemistry^{8,9} and photography¹⁰. Due to the high electronegativity of halogen atoms, significant charge transfer occurs between the Ag surface and adsorbed halogens, resulting in a quasi-ionic metal halogen bond¹¹. Theoretical data, however, suggest that the physical nature of the halogen adatom cannot be understood in the realm of a simple point charge model but rather represents what has been termed "a polarized negative ion" by Lang and Williams¹¹.

Existing structural models for halogen monolayers on Ag(111) have been deduced from surface extended X-ray absorption fine structure (SEXAFS) and low energy electron diffraction (LEED) measurements¹⁻⁷. LEED analysis of Cl, Br and I monolayers on Ag(111) suggests that these halogens form a $\sqrt{3}\times\sqrt{3}/R30$ structure^{1,3,6,7} at submonolayer coverages. The LEED pattern, however, is weak and diffuse^{3,6,7} for Cl and Br, and to our knowledge, no LEED data are published for F adlayers on Ag(111). SEXAFS data² support the $\sqrt{3}\times\sqrt{3}/R30$ structure deduced for I adlayers from LEED analysis¹. In addition, a "honeycomb vacancy structure" has been proposed on the basis of SEXAFS data^{4,5} to resolve uncertainties in the structure of the Cl adlayer derived from LEED studies^{3,6} in the submonolayer regime.

In the present report, we describe a new chemical method of preparing atomically smooth halogen adlayers (F, Cl, Br and I) on Ag. The adlayers are chemically stable in air over a period of several hours, allowing atomically-resolved real-space structures of these materials to be obtained using scanning tunneling microscopy (STM). The structures of Cl, Br, and I adlayers obtained by STM are *consistent* with previous LEED and SEXAFS data; however, for both Br and Cl adlayers on Ag, STM reveals new atomic-level structural features which are not included in previous structural models deduced from either LEED and SEXAFS.

Experimental Section

Our method of preparing Ag surfaces is adapted from the method developed by Zurawski et. al.¹³, who adsorbed iodine on Pt samples and demonstrated that the halogen adlayer effectively protects the sample from surface contaminants. Spherical Ag samples (1-2 mm in diameter) were prepared by melting one end of a ~2cm piece of Ag wire (99.9985 % purity, 0.5 mm diameter, Aesar/Johnson Mathey) in a H₂/O₂ flame. The spheres were further annealed in a pure H₂ flame for ~60 sec, cooled for ~20 sec in air, and transferred into one of the following solutions: hydrofluoric acid (38 %, Baker) to form F adlayers; hydrochloric acid (38 %, Merck) to form Cl adlayers; hydrobromic acid (48 %, Mallinckrodt) to form Br adlayers; and hydroiodic acid (38%, Merck) or 0.1 M solutions of I₂ in methanol to form I adlayers. After immersion of Ag for 30-300 sec, the samples were rinsed with triply distilled water, dried and mounted in a homebuilt specimen holder for STM studies. (Because of the high solubility of AgF in water, rinsing of these samples was usually omitted or very brief.)

The formation of halogen adlayers, as well as surface contamination, was monitored by Auger electron spectroscopy (PHI 595 SAM, cylindrical mirror analyzer). As shown in Fig. 1a, no measurable oxygen or carbon signal is observed in the Auger electron spectrum of a Cl-covered Ag surface. Similar spectroscopic analysis of Ag samples following immersion in HI, HF or HBr solution also did not yield any detectable oxygen or carbon signal, even after exposure of the prepared sample to ambient air for 2-3 hours. Ag samples which were not immersed in a halogen solution, but which were otherwise prepared in an identical fashion, yielded a significant oxygen Auger signal immediately after cooling (see Fig. 1b). These results indicate that the halogen adlayer effectively prevents the adsorption of expected contaminants such as oxygen. Our results are consistent with UHV studies of Kiskinova et. al.¹⁴ and theoretical arguments of Lang

et. al.¹⁵, that indicate that electronegative adsorbates, such as Cl, prevent the coadsorption of oxygen in UHV environments. However, after ~3 hours exposure to air, we were able to detect an oxygen signal on some halogen-coated Ag samples. Therefore, all STM studies were performed within 2 hours of sample preparation.

Surface coverages (Θ) for Cl, Br, and I were estimated by measuring the respective halogen Auger peak heights in relation to the Ag Auger peak, and correcting for the Auger sensitivities which are derived empirically from the respective silver-halogen salt crystal. For Cl adlayers, the peak ratios varied from 0.3 to 0.6. Since the spot diameter of the electron beam impinging on the surface in the Auger experiments was about 50-100 μm , these ratios represent average coverages; the local coverage obtained from STM images varied considerably (see below). For Ag exposed to methanol/I₂ or concentrated HI solutions, the surface coverage of I, Θ_I , ranges from 0.3 to 1.0. Since a full first layer of I on Ag(111) corresponds to $\Theta_I \sim 0.31$, it appears that multilayers of I are readily formed, even for relatively short exposure times (60 sec). Our measured coverages of adsorbed Br are less accurate, since the Auger sensitivity for Br is extremely low. However, we estimate Θ_{Br} to be 0.5, independent of the immersion time for $t > 30$ sec. F adlayers could not be detected by Auger spectroscopic analysis, most likely because AgF decomposes into Ag and F upon exposure to ultraviolet light with photon energies in excess of $\sim 4\text{eV}$ ^{16,17}, which is generated when the Auger electron beam impinges on the sample surface. However, no discernable oxygen or carbon peaks were observed for samples immersed in the HF solutions, indirectly indicating the formation of a protective F adlayer.

Our experiments were performed using a Nanoscope II^(TM) STM¹², in which the tip is held at virtual ground and the bias voltage V_b is applied to the sample. Experiments were performed in air using mechanically cut Pt(70%)Ir(30%) tips. All images were

recorded in the constant current mode using a scan rate of 8.6 Hz and consist of 400 x 400 data points.

Results and Discussion

Chlorine/Ag(111)

Faceted areas are readily observed on all halogen-covered Ag samples using a low magnification optical microscope. The boundaries of the faceted regions form 60° angles, indicating that the facets expose a crystalline Ag (111) surface. STM images taken within the faceted regions of all halogen-coated Ag samples show atomically flat terraces of width up to ~100 nm. The terraces are separated by monoatomic steps of average height $3.0 \pm 0.2 \text{ \AA}$. These features are readily apparent in the low resolution image of the Cl-coated sample shown in Fig. 2, which is representative of all halogen-coated Ag samples.

The STM image shown in Fig. 3a was obtained in the center of one of the terraces. The surface is characterized by a double row structure of Cl atoms. The double row arrangement, however, is not perfect: closer inspection of the image in Fig. 3a reveals that half of the atomic rows are *not* perfectly straight but rather appear to have a quasi-sinusoidal shape with a periodicity of 3-4 nm. Consequently, regions in which the atoms are arranged in a straight double row arrangement are separated by regions which appear to have a nearly perfect hexagonal packing pattern, hereafter referred to as transition regions. Detailed structures of the double row and transition regions are apparent in higher resolution STM images. For example, the image in Fig. 3b was recorded in a double row region of the area shown in Fig. 3a, whereas the image in Fig. 3c was recorded in a transition region. Note that three unit cells coexist in the transition region (see cell outlines in Fig. 3c).

The ratio of the surface density of Cl atoms to the Ag(111)-surface atom layer density yields an absolute coverage of $\Theta_{\text{Cl}} \sim 0.6$, as can be derived from the images shown in Figs. 3b and 3c. We assume that $\Theta_{\text{Cl}} \sim 0.6$ represents the saturation coverage of Cl on Ag(111) since no higher coverages were observed during numerous experiments. Atomically resolved STM images of the Cl adlayer, as well as for all other halogens (see below), can be reproducibly obtained from sample to sample using different PtIr tips, and are representative of large regions of the surface structure on the faceted regions of the Ag surface.

The three nearest neighbor Cl-Cl distances, measured from STM image in Fig. 3b, are $4.1 \pm 0.1 \text{ \AA}$, $3.3 \pm 0.1 \text{ \AA}$ and $3.8 \pm 0.1 \text{ \AA}$. Comparison of the measured Cl-overlayer interatomic distances with the distances between Ag atoms on the Ag(111) surface (2.88 \AA) indicates that the Cl adlayer is incommensurate with the underlying substrate lattice. The geometric relationship of the Cl adlayer to the underlying (111) substrate is apparent from images of *incomplete* adlayers, which are shown in Figs. 4a and 4b ($\Theta_{\text{Cl}} \sim 0.45$ and $\Theta_{\text{Cl}} \sim 0.3$, respectively). From the image shown in Fig. 4a we conclude that the Cl adlayer grows in rows along the [110] direction: the dark circular regions are assigned to the underlying Ag(111) lattice since they form a hexagonal structure (see outline in Fig. 2d) with a periodicity of $3.1 \pm 0.2 \text{ \AA}$, close to the 2.88 \AA atom spacing in the topmost layer of Ag(111). The difference of $\sim 0.2 \text{ \AA}$ may be due to a slight expansion of the Ag(111) lattice under the influence of Cl chemisorption, consistent with the fact that the surface atom density in AgCl(111) is significantly lower than on Ag(111) (7.3 atoms per 100 \AA in AgCl(111) vs. 13.8 atoms per 100 \AA in Ag(111)).

The bright circular regions in Fig. 4a represent Cl atoms with nearest neighbor distances of $6.2 \pm 0.2 \text{ \AA}$, $4.1 \pm 0.2 \text{ \AA}$, $3.3 \pm 0.2 \text{ \AA}$ and $3.8 \pm 0.2 \text{ \AA}$. The row structure along the [110] direction is immediately obvious, even though some atoms are not perfectly aligned and disordered. At $\Theta_{\text{Cl}} \sim 0.3$ (Fig. 4b), every second row of the

structure shown in Fig. 3b is missing and the interatomic distances are $4.1 \pm 0.1 \text{ \AA}$ along the $[110]$ direction and $6.2 \pm 0.1 \text{ \AA}$ along the $[112]$ direction.

In order to compare our (real space) STM results with (reciprocal space) LEED patterns, we constructed the reciprocal lattices from our STM images (see, e.g., the procedure described in ref. 18). It is clear from the images in Fig. 3 ($\Theta_{\text{Cl}} = 0.6$) that the three different adlayer unit cells outlined in the image presented in Fig. 3c, and schematically depicted in Fig. 5, coexist in surface areas as small as $\sim 15 \text{ nm}^2$. Since the dimensions of this area are clearly smaller than the transfer width of the electron beam in a typical LEED experiment¹⁸, LEED will sample all three cells *coherently*. Therefore, at saturation coverage the LEED pattern will result from an average of the three patterns, which is equivalent to the unit cell corresponding to the transition region, Fig. 5c. The resulting LEED pattern constructed from this pattern is depicted in Fig. 5d. Apart from a slight mismatch (see below), the LEED pattern observed by Bowker Waugh³ at saturation coverage is essentially identical to that constructed from the STM images. The mismatch arises because the two unit cell vectors in Fig. 5c are of slightly different length (4.1 \AA and 3.8 \AA). Bowker and Waugh³ interpreted their LEED pattern assuming a complete Cl monolayer with a Cl atom density equal to that in AgCl(111) (i.e., 4.1 \AA Cl-Cl nearest neighbor distance). This discrepancy can be readily explained as follows.

Since we observe a row structure of Cl atoms along one of the three principal symmetry axes of the hexagonal Ag(111) surface, we conclude that *three domains* of Cl atom rows may exist on extended Ag(111) surface areas. One domain, however, may prevail throughout one facet. Since STM samples a small surface area, the probability of obtaining atomically resolved images of surface regions which show two or three domains is extremely small. We did not observe any in our study. The physical diameter of the electron beam in a LEED experiment, on the other hand, is of the order of $\sim 1 \text{ mm}$. Therefore, the actual LEED pattern consists of superimposed diffraction spots resulting

from different domains (see, e.g., ref. 18) which, in case of a (111) surface, are rotated by 120° with respect to each other. Considering this effect, the LEED pattern constructed from the unit cell in Fig. 5c has to be rotated by two consecutive 120° rotations and the three resulting patterns have to be added so as to simulate the LEED experiment. It is clear then, that the slight mismatch of 0.3 \AA in one lattice direction will not be apparent in the measured LEED pattern. We conclude that the STM images in Fig. 3 and the LEED pattern of Bowker and Waugh³ and Goddard and Lambert⁶ at saturation coverage are in excellent agreement.¹⁹

At low Cl coverages, a very weak and diffuse $\sqrt{3}\times\sqrt{3}/R30$ pattern is observed in LEED^{3,6}. From the STM data in Fig. 4b ($\Theta_{\text{Cl}} = 0.3$), we again construct the unit cell and the expected LEED pattern as depicted in Figs. 6a and 6c, respectively²⁰. Also shown is the two dimensional fourier power spectrum computer generated from the image in Fig. 4b (Fig. 6b). Note that the components of the underlying Ag(111) lattice form a hexagonal spot pattern with a periodicity of $3.1 \pm 0.2 \text{ \AA}$ in the fourier spectrum. The substrate atoms do not appear in the real space image.

Applying again the argument that the actual LEED pattern will consist of diffraction emerging from different domains, we rotated the pattern in Fig. 6c by two consecutive 120° rotations generating the three patterns shown in Fig. 6d. The sum of these three patterns is shown in Fig. 6d, which is qualitatively similar to the weak and diffuse $\sqrt{3}\times\sqrt{3}/R30$ pattern observed in LEED. Since it is reasonable to assume that the degree of disorder in the adlayer is highest at low coverages (i.e., $\Theta_{\text{Cl}} = 0.3$), a quasi- $\sqrt{3}\times\sqrt{3}/R30$ pattern may only be observed in LEED at slightly higher coverages. Bowker and Waugh³ report that the coverage, at which the $\sqrt{3}\times\sqrt{3}/R30$ LEED pattern is first observed amounts to ~ 0.8 of a Cl-monolayer. Since $7.3 \text{ atoms per } 100 \text{ \AA}^2$ is the atom density found on AgCl(111), these authors assumed that this atom density is also found at full Cl coverage. Therefore, a completed Cl-monolayer translates in their work into an

absolute coverage of $\Theta_{\text{Cl}} \sim 0.55$. Our work shows that the monolayer is complete at a coverage $\Theta_{\text{Cl}} \sim 0.6$. In summary, we emphasize that all observed LEED patterns for the Cl/Ag(111) system can be well understood on the basis of our STM images²¹. However, the actual physical structure deduced from LEED analysis is inconsistent with the real-space, atomically resolved STM images.

As a final note regarding the Cl adlayer structure, it is interesting to consider the "honeycomb vacancy structure" for the Cl adlayer on Ag(111), proposed by Lamble et al.^{4,5} based on LEED and SEXAFS measurements. This unusual structure has nearest neighbor Cl-Cl distances of 2.9 Å and 5.0 Å. In addition to these values, the transformed SEXAFS spectrum, which is presented in refs. 4 and 5, and which gives the distribution of interatomic distances in the surface layer, shows additional strong peaks occurring at ~ 3.2 Å, 3.9 Å and 4.2 Å (the peaks at 2.9 and 5.0 Å which were used in the original structural analysis appear only as weak shoulders). We therefore suggest that the SEXAFS data should be reinterpreted with the peaks at 3.2 Å, 3.9 Å and 4.2 Å assigned to interatomic distances within the Cl adlayer, in good agreement with values obtained from STM in the coverage range from $\Theta_{\text{Cl}} \sim 0.45$ to $\Theta_{\text{Cl}} \sim 0.6$ (3.3 ± 0.1 Å, 3.8 ± 0.1 Å, 4.1 ± 0.1 Å and 6.2 ± 0.1 Å).

Flourine/Ag(111)

The double row structure observed for F adlayers on Ag(111), shown in Fig 7a., is very similar to that for Cl. However, the interatomic distances reflect a compression of the atoms within each double row; the three nearest neighbor distances are 2.8 ± 0.1 Å, 3.0 ± 0.1 Å and 4.2 ± 0.1 Å. The saturation coverage corresponding to a completed double row structure, $\Theta_{\text{F}} \sim 0.7$, is therefore slightly higher than that for Cl. Assuming that the rows are oriented along the [110] direction, models of the F adlayer structure on

Ag(111) suggest that the adsorption sites in the double row arrangement alternate between three-fold hollow and two-fold bridge sites in adjacent rows.

Bromine/Ag(111)

The monolayer structure for Br (Fig. 7b) is best characterized as intermediate between the $\sqrt{3}\times\sqrt{3}/R30$ structure of the I monolayer (see below) and the double row structures of F and Cl. The absolute coverage, Θ_{Br} , for the saturated monolayer shown in Fig. 7b is ~ 0.45 , the three interatomic distances are $5.3 \pm 0.1 \text{ \AA}$, $5.1 \pm 0.1 \text{ \AA}$ and $4.4 \pm 0.1 \text{ \AA}$. Assuming the same growth pattern on three different domains for Br on Ag(111) as for Cl and performing the same analysis, a quasi- 3×3 LEED pattern similar to that observed by Goddard et. al.⁷ is readily constructed from the STM image in Fig. 7b. A quasi- $\sqrt{3}\times\sqrt{3}/R30$ LEED pattern is expected to occur at slightly lower coverages $\Theta_{\text{Br}} \sim 0.35$. Goddard et. al.⁷ observed such a pattern for Br on Ag(111), which was diffuse and weak as in the case for Cl adlayers.

Iodine/Ag(111)

The structure of the I monolayer on Ag(111) ($\Theta_{\text{I}} \sim 0.3$) closely resembles a true $\sqrt{3}\times\sqrt{3}/R30$ adlayer structure (Fig. 7c) with interatomic distances in the outlined cell of $4.9 \pm 0.1 \text{ \AA}$ and $4.6 \pm 0.1 \text{ \AA}$. The apparent slight compression of the adlayer lattice in one crystallographic direction may be related to the row structure growth observed for the smaller halogens. Considering that again three different domains coexist on extended surface areas, the small mismatch is expected to average out in LEED and SEXAFS experiments. The structure observed in our STM images and those obtained from earlier LEED¹ and SEXAFS² measurements are in excellent agreement. We note that the I-adlayer structure resulting from exposure of Ag to molecular iodine dissolved in methanol is identical to that obtained by exposure to concentrated HI solutions.

Conclusions

The method of synthesizing halogen adlayers on Ag(111) that we have described allows detailed structural characterization of these surfaces in air by STM. The observed Cl, Br and I monolayer structures are entirely *consistent* with previous LEED and SEXAFS *data*. The structures deduced from LEED and SEXAFS, however, need to be revised for the Cl and Br adlayers.

Our images show that the relative degree of symmetry within the halogen monolayer structure increases with decreasing adatom electronegativity and increasing adatom size. We conclude, that the actual adsorbate layer structure depends on the local *charge distribution* within the metal-halogen complex and on the *size* of the halogen atom. Thus the atomic arrangements of the F, Cl and Br monolayers on Ag(111) may reflect non-spherical lateral coulombic forces between localized charges around neighboring adatoms. For I, essentially the same local charge distribution is expected. However, in comparison to F or Cl, the relative degree of charge localization for I, and, hence, the degree of polarization, is expected to be lower. This trend is also seen in X-ray diffraction studies of solid halogens²². In a Cl₂ crystal, for example, the nearest neighbor atomic distances are found to be spacially highly anisotropic. It is this property of the halogens that may be responsible for the row structures seen in STM images.

Acknowledgements

The authors thank D.Z. Liu for performing the Auger spectroscopic analyses and Prof. M.D. Ward helpful discussions. This work was supported by the Office of Naval Research. J.H.S gratefully acknowledges partial support from the Deutsche Forschungsgemeinschaft, grant no. Sch 428/1-1.

References

1. Forstman, F.; Berndt, W.; Büttner, P. *Phys. Rev. Lett.* **1973**, 30(1), 17-19
2. Citrin, P.H.; Eisenberger, P.; Hewitt, R.C. *Phys. Rev. Lett.* **1978**, 41(5), 309-312
3. Bowker, M.; Waugh, K.C. *Surf. Sci.* **1983**, 134, 639-664
4. Lamble, G.M.; Brooks, R.S.; Ferrer, S.; King, D.A. *Phys. Rev. B.* **1986**, 34(4), 2975-2978
5. Lamble, G.M.; King, D.A. *Phil. Trans. R. Soc. Lond. A* **1986**, 318, 203-207
6. Goddard, P.J.; Lambert, R.M. *Surf. Sci.* **1977**, 67, 180-194
7. Goddard, P.J.; Schwaha, K.; Lambert, R.M. *Surf. Sci.* **1978**, 71, 351-363
8. Valette, G.; Hamelin, A.; Parsons, P. *Z. Phys. Chem. N.F.* **1978**, 113, 71-89
9. Birss, V.I.; Smith, C.K. *Electrochimica acta* **1987**, 32(2), 259-268
10. Hamilton, J.F.; *Advances in Physics* **1988**, 37(4), 359-441
11. Lang, N.D.; Williams, A.R. *Phys. Rev. B* **1978**, 18(2), 616-636
12. Digital Instruments, Inc., Nanoscope II Manual
13. Zurawski, D.; Rice, L.; Hourani, M.; Wieckowski, A. *J. Electroanal. Chem.* **1987**, 230, 221-231
14. Kiskinova, M.; Goodman, D.W. *Surf. Sci.* **1981**, 108, 64-76
15. Lang, N.D.; Holloway, S.; Nørskov, J.K. *Surf. Sci.* **1985**, 150, 24-38
16. Zmbov, K.F.; Margrave, J.L. *J. Phys. Chem.* **1967**, 71, 446-448
17. Clements, R.M.; Barrow, R.F. *Chemical Communications* **1968**, 1, 27-28
18. Ertl, G.; Küppers, J. *Low Energy Electrons and Surface Chemistry*; VCH Verlagsgesellschaft mbH, Weinheim, Germany 1985; pp. 201 -226
19. Our STM images in Fig. 3 also explain the split spot LEED pattern observed by Bowker and Waugh³ slightly before completion of the monolayer. At a coverage slightly below $\Theta_{C1} = 0.6$ the unit cells shown in Fig. 5a and 5b may coexist

within the transfer width of the LEED beam, resulting in a split spot diffraction pattern.

20. The LEED pattern for the image in Fig. 4a, $\Theta_{\text{Cl}} \sim 0.45$, will only slightly differ from the one depicted in Fig. 6 in that it will contain weak components of the high coverage LEED pattern shown in Fig.5.
21. Since STM is sensitive to the surface of a sample, the dissolution of Cl in the bulk of the Ag crystal, as suggested by Bowker and Waugh³ can not be ruled out on the basis of our results.
22. Collin, R.L. *Acta Cryst.* 1952, 5, 431-432

Figure Captions

Figure 1. Auger electron spectra of Ag samples: a) Cl-coated Ag; b) Ag sample, cooled in air. Note the absence of the oxygen peak at 550 eV in the Cl-coated sample.

Figure 2. Low resolution STM image of a Cl-coated sample, showing terraces separated by monoatomic steps. Note the numerous kink sites at the steps separating different terraces. ($V_b = -850$ mV, $i_t = 2.3$ nA). Unfiltered data.

Figure 3. a) Unfiltered atomically resolved STM image of the Cl monolayer on Ag (111). The double row arrangement is faulted by slip defects with a periodicity of ~ 2 -3 nm; ($V_b = -1085$ mV, $i_t = 4.3$ nA). b) Band-pass filtered defect free portion of the area shown in Fig. 3a; the adlayer unit cell is outlined. $\Theta_{Cl} \sim 0.6$. ($V_b = -995$ mV, $i_t = 4.6$ nA). c) Band-pass filtered portion of the surface area shown in Fig. 3a, featuring the slip defect. Note that only every second row slips, whereas the other rows are unaffected. The three unit cells of the Cl adlayer are outlined. $\Theta_{Cl} \sim 0.6$. ($V_b = -1005$ mV, $i_t = 4.6$ nA).

Figure 4. a) Low pass filtered image of incomplete Cl adlayer ($\Theta_{Cl} \sim 0.45$). The dark spots represent the underlying Ag(111) surface atoms. The hexagonal substrate unit cell is outlined. The bright spots represent Cl atoms. ($V_b = -680$ mV, $i_t = 5.5$ nA). b) Band pass filtered image of the incomplete Cl adlayer ($\Theta_{Cl} \sim 0.3$). The unit cell is outlined. ($V_b = -785$ mV, $i_t = 4.2$ nA).

Figure 5 a,b,c). The three real space unit cells (solid lines) of the Cl adlayer that occur in the images shown in Fig. 3 and (d) the corresponding LEED pattern constructed from geometric diffraction theory. The unit cell of the Ag(111) is also shown (broken lines).

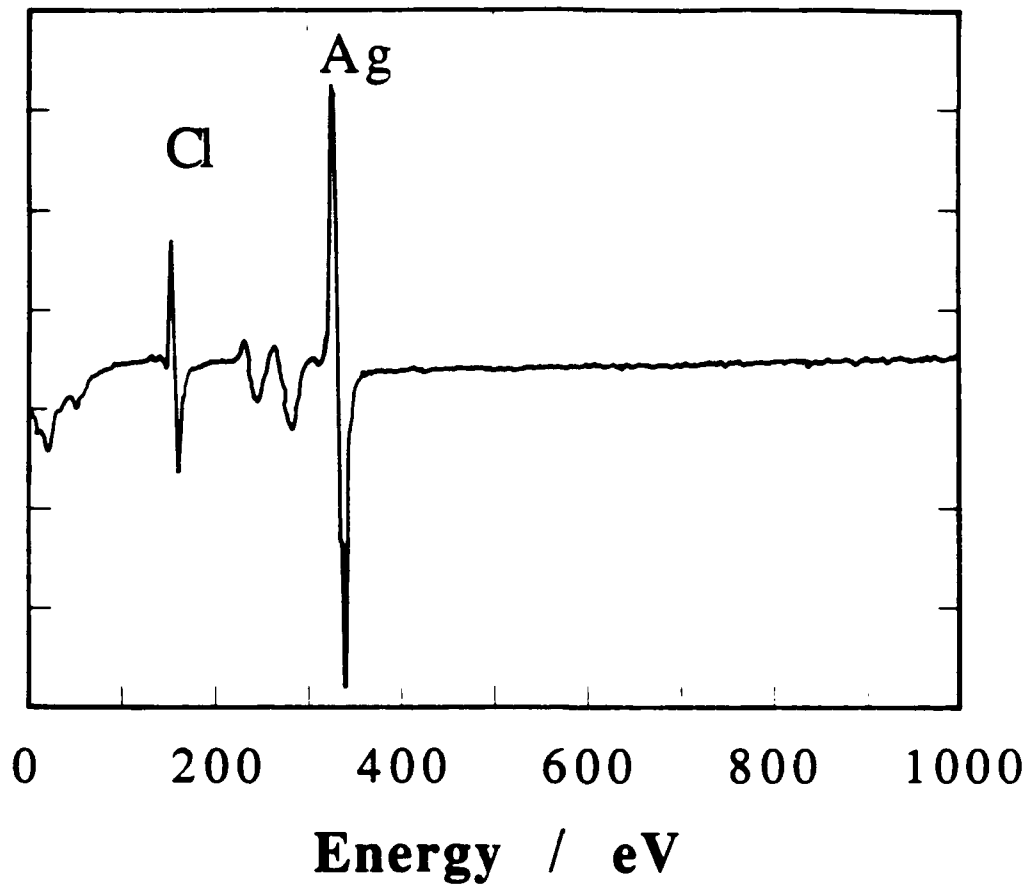
The crosses represent real space atomic positions and diffraction spots from the Ag(111) substrate. The open circles represent real space positions and diffraction spots corresponding to the Cl adlayer. Note that the unit cell (c) represents the geometric average of the units cells (a), (b) and (c); therefore only the LEED pattern corresponding to cell (c) is constructed in Fig. 5d. (see text).

Figure 6. a) The Cl adlayer unit cell, (b) the corresponding two dimensional fourier power spectrum computer generated from the image in Fig. 4b, and (c) the LEED pattern for low Cl coverages. The symbols are the same as in Fig. 5. Since the rows are oriented along one of the principal symmetry axis of the (111) surface, three domains rotated by 120° with respect to each other are expected to coexist on extended surface areas. The actual LEED pattern is then a superposition of the three patterns and is shown in (d). The sum-pattern explains the experimentally observed weak and diffuse $\sqrt{3}\times\sqrt{3}/R30$ LEED pattern which is schematically depicted in Fig. 6e.

Figure 7. Atomically-resolved STM images of halogen adlayers on Ag(111): a) F adlayer, $\Theta_F \sim 0.7$ ($V_b = -1135$ mV, $i_t = 2.2$ nA); b) Br adlayer, $\Theta_{Br} \sim 0.45$ ($V_b = -550$ mV, $i_t = 5.7$ nA); c) I adlayer, $\Theta_I \sim 0.3$. ($V_b = -358$ mV, $i_t = 4.9$ nA).

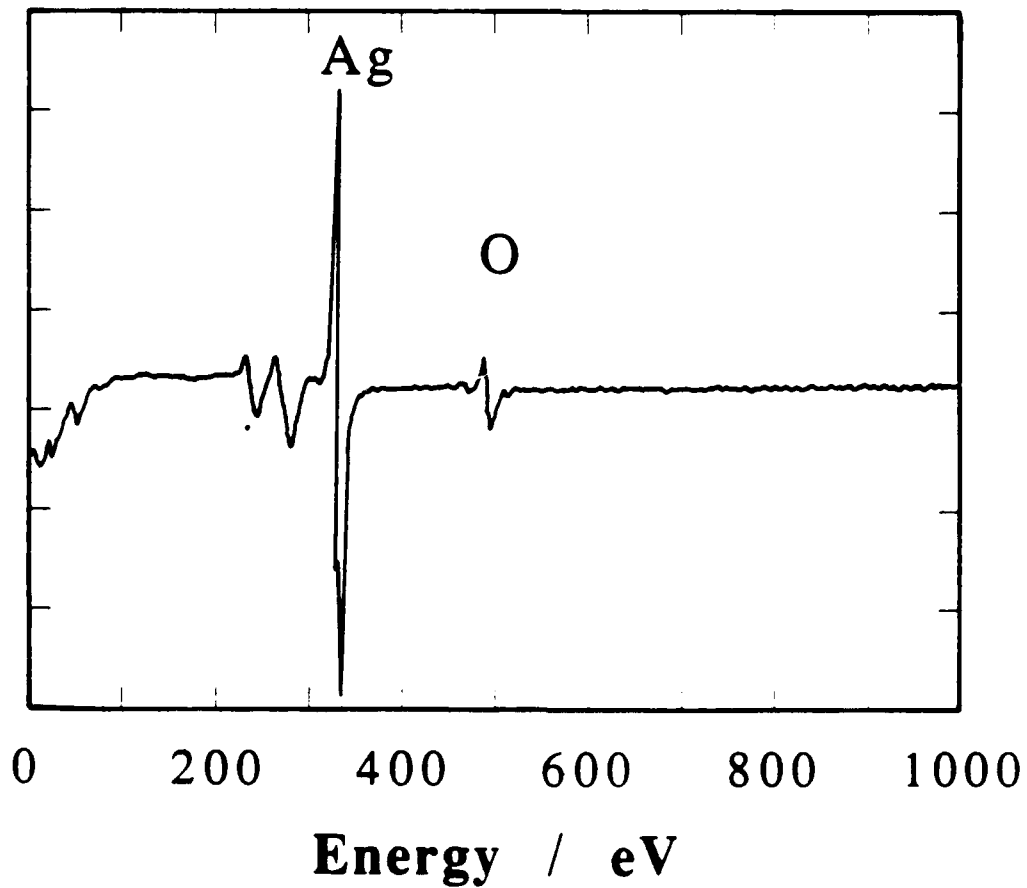
a

$\frac{dN(E)}{dE} / \text{a.u.}$



b

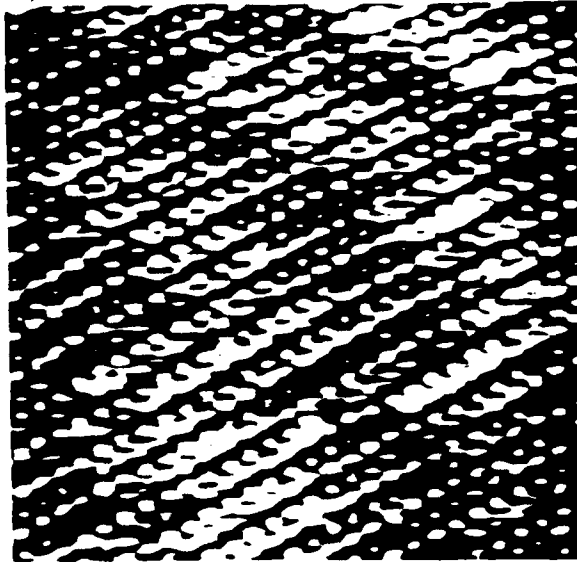
$\frac{dN(E)}{dE} / \text{a.u.}$



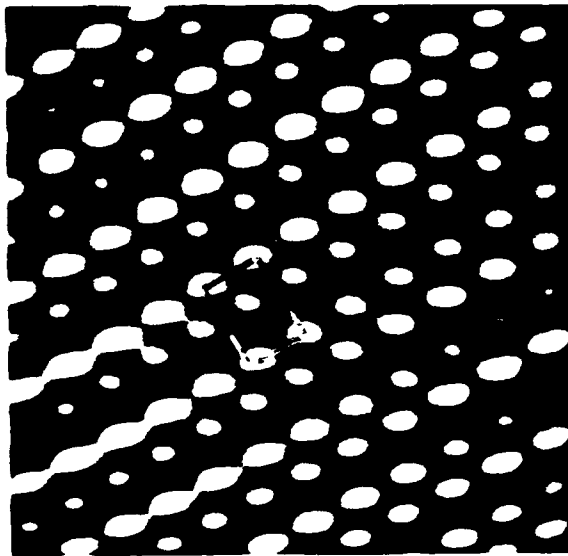
50 x 50 nm²



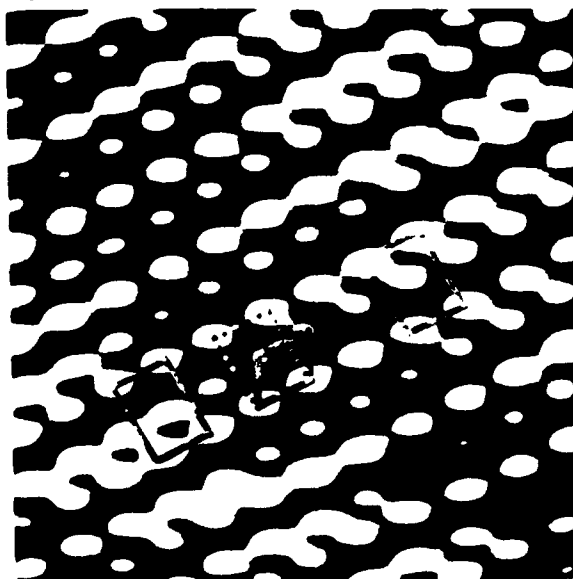
a) $10 \times 10 \text{ nm}^2$



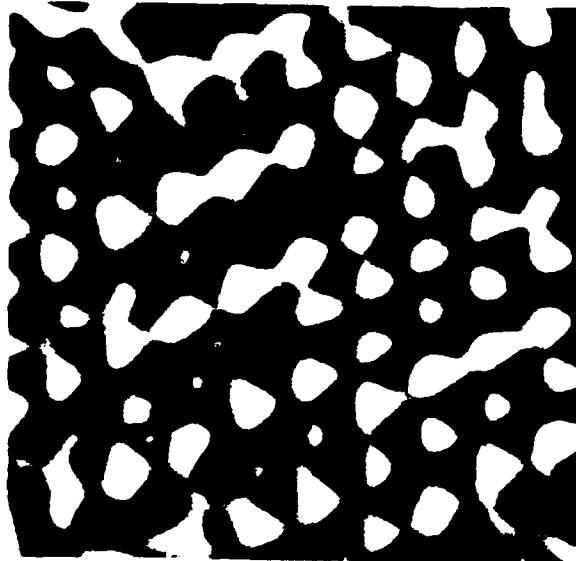
b) $6 \times 6 \text{ nm}^2$



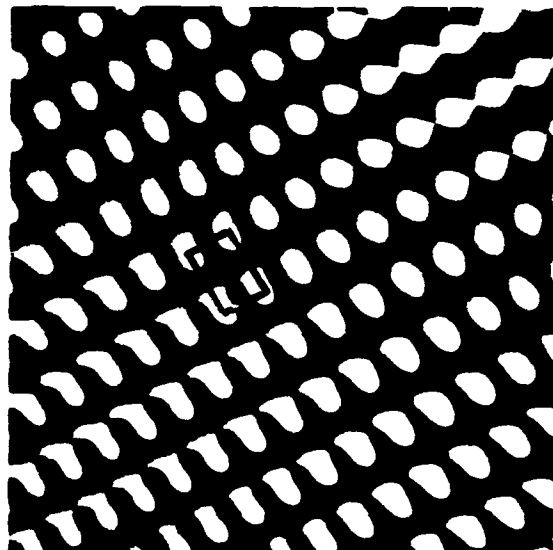
c) $6 \times 6 \text{ nm}^2$

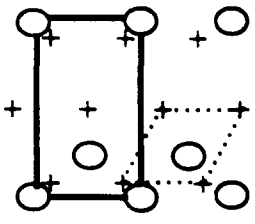
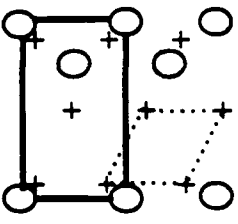
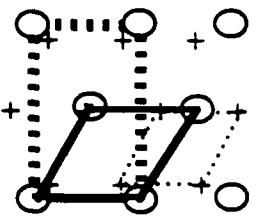
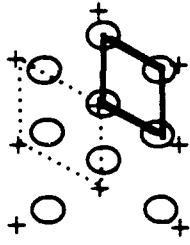


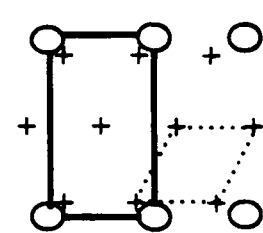
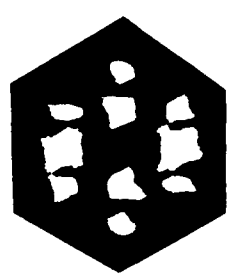
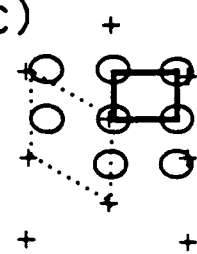
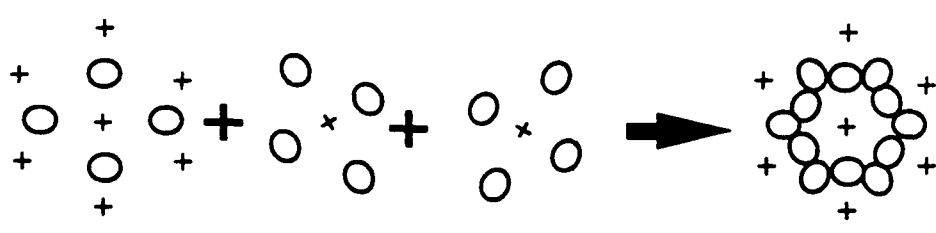
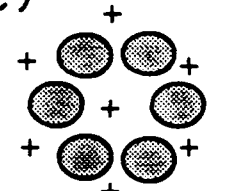
a) $3.4 \times 3.4 \text{ nm}^2$



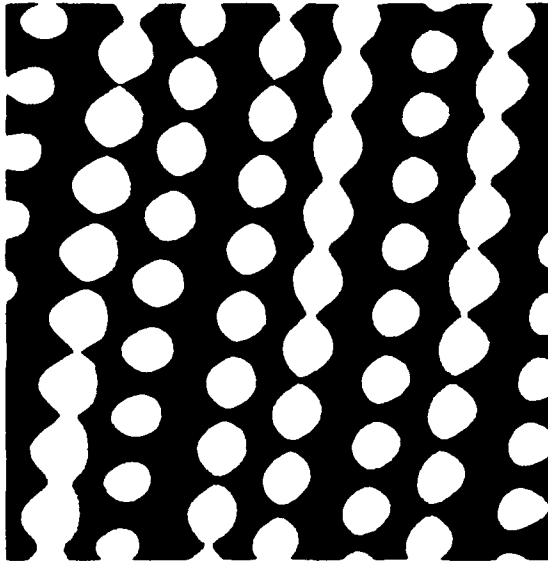
b) $5.7 \times 5.7 \text{ nm}^2$



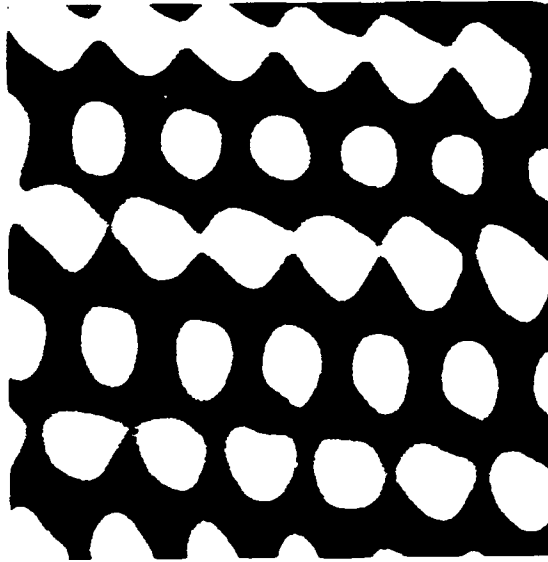
Unit cells (real space) $\theta_{c1} = 0.6$	LEED
<div style="display: flex; justify-content: space-around; align-items: center;"> <div style="text-align: center;">  <p>a)</p> </div> <div style="text-align: center;">  <p>b)</p> </div> <div style="text-align: center;">  <p>c)</p> </div> </div>	<div style="text-align: center;">  <p>d)</p> </div>

$\theta_{c1} = 0.3$		LEED
<p>a)</p> 	<p>b)</p> 	<p>c)</p> 
<p>d)</p> 		<p>e)</p>  <p>observed</p>

a) $2.5 \times 2.5 \text{ nm}^2$



b) $2.5 \times 2.5 \text{ nm}^2$



c) $2.5 \times 2.5 \text{ nm}^2$

